Available online at www.sciencedirect.com
SCIENCE DIRECT®
Journal of Organometallic Chemistry 673 (2003) 56–66
Journal of Organometallic Chemistry
www.elsevier.com/locate/jorganchem

A density functional theory study of dinitrogen bonding in ruthenium complexes

Ridha Ben Said [a], Khansaa Hussein [b,1], Bahoueddine Tangour [a], Sylviane Sabo-Etienne [c], Jean-Claude Barthelat [b,*]

[a] Unité de Recherche de Physico-Chimie Moléculaire, Institut Préparatoire des Etudes Scientifiques et Techniques (IPEST), Boite Postale 51, 2070 La Marsa, Tunisia
[b] Laboratoire de Physique Quantique, IRSAMC (UMR 5626), Université Paul Sabatier, 118 Route de Narbonne, 31062 Toulouse Cedex 04, France
[c] Laboratoire de Chimie de Coordination du CNRS, 205 Route de Narbonne, 31077 Toulouse Cedex 04, France

Received 13 January 2003; accepted 13 March 2003

Abstract

Dinitrogen ruthenium complexes were theoretically studied by means of DFT technique. Several isomers of $RuH_2(N_2)(PH_3)_2$, $RuH_2(N_2)_2(PH_3)_2$ and $RuH_2(H_2)(N_2)(PH_3)_2$ were studied. Calculations of relative energies, geometrical parameters, vibrational frequencies and natural orbital bond analysis were performed. It is shown that the most stable isomer for each series is characterized by a *trans* position of the phosphines with the dinitrogen ligand *trans* to one hydride. As usually observed, the dinitrogen moiety adopts an end-on bonding mode and is weakly elongated from free N_2 (generally not $>1\%$). As shown by NBO analysis, such a bonding mode involves σ-donation of about 0.2 electron from the lone pair orbital of the ruthenium-bound nitrogen toward ruthenium and back-donation of roughly 0.2 electron from the 4d occupied orbital of ruthenium to the two π_g^* dinitrogen orbitals.

Keywords: DFT calculations; Dinitrogen complexes; Dihydrogen complexes; Ruthenium

1. Introduction

The coordination of dinitrogen on a metal centre continues to attract a lot of interest as models for nitrogenase, to achieve ammonia production, or to form metal-nitrido compounds for material science [1]. Since the discovery in 1965 of the first dinitrogen complex $[Ru(N_2)(NH_3)_5]^{2+}$ [2], dinitrogen compounds of nearly each transition element have been prepared [3–5]. Among the various bonding modes of N_2 to a metal centre, the terminal end-on type is predominant. The majority of dinitrogen compounds displays a dinitrogen moiety (≈ 1.12 Å) that is not significantly elongated from free N_2 (1.097 Å), and dinitrogen can be considered as weakly activated. End-on bonding can be described similarly for N_2 and CO, by involving both σ-donation from the N_2 moiety to the metal and π back-bonding from the metal to the two orthogonal N_2 π*-orbitals.

It is noteworthy that dinitrogen complexes also play a role in the chemistry of dihydrogen complexes as a tool for the prediction of the stability of the dihydrogen coordination [6,7]. The measurements of ν_{NN} and electrochemical potentials are indicators of π basicity of the binding site in $M(N_2)L_n$ complexes. It is generally admitted that a value of ν_{NN} greater than 2060 cm^{-1} will be in favour of the formation of a dihydrogen complex whereas lower values will indicate the formation of a dihydride as a result of oxidative addition.

Some of us have extensively studied the properties of the thermally stable bis(dihydrogen) complex $RuH_2(H_2)_2(PCy_3)_2$ [8]. Theoretical studies have shown that the bis(dihydrogen) complex has three isomeric structures within an energy range of only 2 kcal mol^{-1} in agreement with the high fluxionality of this molecule [9]. The geometry of the lowest energy isomer corresponds

* Corresponding author. Tel.: +33-5-61556559; fax: +33-5-61556065.
E-mail address: barthelat@irsamc.ups-tlse.fr (J.-C. Barthelat).
[1] Present address: Department of Chemistry, Faculty of Sciences, University Al-Baath, Homs, Syria.

0022-328X/03/$ - see front matter
doi:10.1016/S0022-328X(03)00157-8

to the structure recently determined by X-ray analysis [10]. The analogous bis(dinitrogen) complex $RuH_2(N_2)_2(PCy_3)_2$ was synthesized and characterized by IR and NMR data, but could not be isolated [11]. In the case of the triisopropylphosphine analogue, the reaction of dinitrogen with $RuH_2(H_2)_2(P^iPr_3)_2$, leads to the formation of a dinuclear complex $\{RuH_2(N_2)(P^iPr_3)_2\}_2(\mu\text{-}N_2)$ which was isolated and characterized by X-ray [12]. In solution, an equilibrium mixture of the dimer and the mononuclear species $RuH_2(N_2)_2(P^iPr_3)_2$ was detected by NMR.

We now report a theoretical study of several isomers resulting from the coordination of dinitrogen on the ruthenium fragment $RuH_2(PH_3)_2$. Three series of isomers i.e., $RuH_2(N_2)(PH_3)_2$, $RuH_2(N_2)_2(PH_3)_2$ and $RuH_2(H_2)(N_2)(PH_3)_2$ have been investigated, allowing a comparison between dihydrogen and dinitrogen fixation.

2. Computational details

The theoretical treatment of the different systems included in this work was performed by using the DFT/B3LYP approach implemented in the GAUSSIAN98 series of programs [13]. The B3LYP hybrid functional [14] has been found to be quite reliable in describing potential energy surfaces (PES) and binding energies in ruthenium complexes [8c,9,15].

For ruthenium, the core electrons were represented by a relativistic small-core pseudo-potential determined according to the Durand–Barthelat method [16]. The 16 electrons corresponding to the 4s, 4p, 4d, and 5s atomic orbitals were described by a (7s, 6p, 6d) primitive set of Gaussian functions contracted to (5s, 5p, 3d). Standard pseudo-potentials developed in Toulouse were used to describe the atomic cores of nitrogen and phosphorus [17]. A double-zeta plus polarization valence basis set was employed for each atom (d-type function exponents were 0.95 and 0.45, respectively). For hydrogen, a standard (4s) primitive basis contracted to (2s) was used. A p-type polarization function (exponent 0.90) was added for the hydrogen atoms directly bound to ruthenium.

The geometries of the different species under consideration were optimized using analytic gradient. The harmonic vibrational frequencies of the different stationary points of the PES have been calculated at the same level of theory in order to identify the local minima as well as to estimate the corresponding zero point vibrational energy (ZPE). The transition state was confirmed by frequency calculations and intrinsic reaction coordinate (IRC) calculations. Binding energies were also calculated by using MPn perturbative methods and the more accurate CCSD(T) method using the DFT/B3LYP optimized geometries. The nature of dinitrogen bonding was analyzed using natural bond orbital NBO calculations [18].

3. Results and discussion

Three series of isomers $RuH_2(N_2)(PH_3)_2$, $RuH_2(N_2)_2(PH_3)_2$ and $RuH_2(H_2)(N_2)(PH_3)_2$ resulting from the coordination of N_2 to the ruthenium fragment $RuH_2(PH_3)_2$ have been studied (see Scheme 1). We will first describe the geometries of the different optimized isomers with their relative energies. The discussion will be followed by a thermodynamic analysis and a NBO study.

3.1. The mono(dinitrogen) complex $RuH_2(N_2)(PH_3)_2$

We can consider the mono(dinitrogen) complex $RuH_2(N_2)(PH_3)_2$ (**1**) as a distorted octahedron where the ligands (two hydrides, two phosphines and the dinitrogen ligand) are placed on five vertices among the six available. $RuH_2(N_2)(PH_3)_2$ is a 16-electron species with a vacant site remaining in the pseudo-octahedral environment around the ruthenium atom (see Equation 1 in Scheme 1). The different isomers were denoted with respect to the relative position of the phosphines: **T** for *trans* and **C** for *cis*. They are depicted in Fig. 1. In isomers where phosphines are *trans* to each other, two possibilities can occur, depending on the position of the two hydrides: the corresponding isomer will be noted **1Ta** for a *cis* position and **1Tb** for a *trans* position. In the case where the two phosphines are *cis* to each other, the dinitrogen ligand can occupy three different positions: *trans* to a phosphine, a hydride or a vacant site. The corresponding isomers will be noted **1Ca**, **1Cb** and **1Cc**, respectively.

All these isomers were optimized by means of the DFT/B3LYP method. As expected, optimization of **1Tb** could not be obtained, the process leading to **1Ta**. This is the result of the unfavourable *trans* position of the two strong σ-donor hydrides. The other four isomers **1Ta**, **1Ca**, **1Cb**, **1Cc** have been identified as local minima on the singlet PES. Optimized values of selected geometrical parameters are listed in Table 1. In all isomers, Ru, N1 and N2 are nearly in line, the Ru–N1–

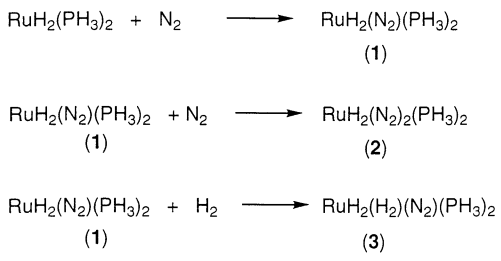

Scheme 1.

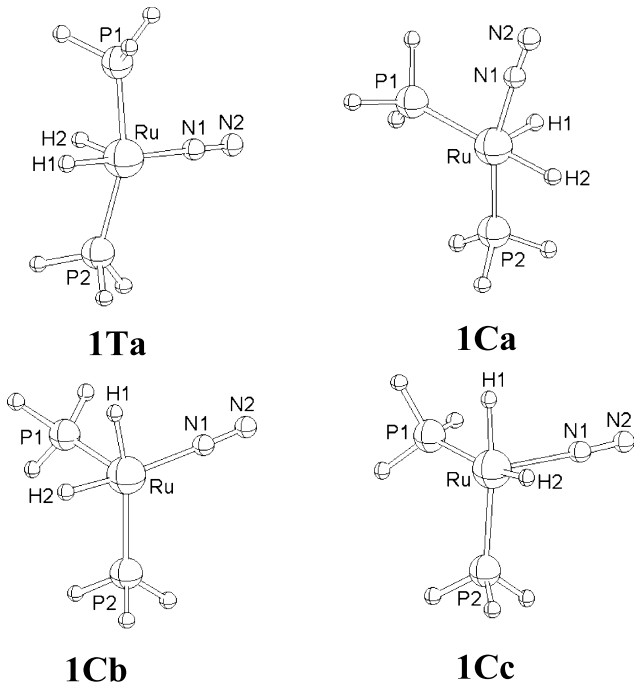

Fig. 1. DFT/B3LYP-optimized geometries of $RuH_2(N_2)(PH_3)_2$ isomers (**1**).

Table 1
Selected optimized geometrical parameters [a] for the four isomers of $RuH_2(N_2)(PH_3)_2$ calculated at the DFT/B3LYP level of theory

	1Ta (C_s)	**1Ca** (C_1)	**1Cb** (C_1)	**1Cc** (C_1)
Ru–H1	1.666	1.599	1.624	1.638
Ru–H2	1.651	1.639	1.617	1.634
Ru–N1	2.311	2.206	2.060	2.166
N1–N2	1.152	1.123	1.121	1.123
Ru–P1	2.386	2.394	2.192	2.398
Ru–P2	2.386	2.327	2.389	2.396
P1–Ru–P2	157.3	85.9	101.0	98.5
H1–Ru–H2	85.5	91.0	82.4	85.4
H1–Ru–P1	81.5	89.5	79.8	86.0
H2–Ru–P1	86.1	175.2	81.9	166.4
H1–Ru–P2	81.5	85.8	167.6	166.4
H2–Ru–P2	86.1	79.3	85.5	86.0
H1–Ru–N1	178.7	88.9	90.7	86.2
H2–Ru–N1	91.4	86.4	172.6	86.2
N1–Ru–P1	98.4	95.6	99.7	96.6
N1–Ru–P2	98.4	165.0	101.2	96.6
Ru–N1–N2	177.8	178.4	177.5	178.1

[a] Distances are in angstrom (Å) and angles in degrees (°).

N2 angle being roughly equal to 180°. This geometry indicates that the N_2 ligand adopts an end-on bonding mode which is the most commonly encountered in dinitrogen compounds. All attempts to optimize a side-on structure have failed.

The relative energies as well as corrections of zero point energy (ZPE) and thermal enthalpy are gathered in Table 2. Whatever the thermodynamic variable we consider, **1Ta** is the most stable isomer. For isomers of type **1C**, **1Ca** is only 2.9 kcal mol^{-1} less stable than **1Ta**. The two other isomers, **1Cb** and **1Cc**, are calculated to be higher in energy.

Table 2
DFT/B3LYP relative energies (kcal mol^{-1}) of $RuH_2(N_2)(PH_3)_2$ isomers

Isomer	ΔE	ΔE+ZPE	ΔH°	ΔG°
1Ta	0.0	0.0	0.0	0.0
1Ca	3.0	2.9	2.9	2.9
1Cb	9.6	9.7	9.6	9.6
1Cc	18.8	18.6	18.6	18.4

In the most stable isomer (**1Ta**), the vacant site is *trans* to one hydride and the N–N distance of 1.152 Å is the longest observed in this series. It is lengthened by 4.0% compared to the bond length in free N_2 (1.108 Å) calculated at the same level of theory. Similar but less important elongation has been observed for isomers **1Ca**, **1Cb** and **1Cc** for which the N–N bond lengths are roughly around 1.12 Å. This testifies of a weak activation of the N_2 ligand by the complexation process. It is interesting to note a good correlation between the position of the vacant site and the corresponding shortening of the Ru–X bond distance *trans* to this vacant site. Indeed, Ru–H1 distance reduces from 1.638Å (**1Cc**) to 1.599Å (**1Ca**), Ru–N1 from 2.206Å (**1Ca**) to 2.166Å (**1Cc**) and Ru–P1 from 2.394Å (**1Ca**) to 2.192Å (**1Cb**).

While comparing the relative energies and the geometrical parameters, we can conclude that the dinitrogen ligand prefers a *trans* position to a hydride, whereas the position *trans* to the vacant site is energetically unfavourable.

3.2. The bis(dinitrogen) complex $RuH_2(N_2)_2(PH_3)_2$

The bis(dinitrogen) complex $RuH_2(N_2)_2(PH_3)_2$ (**2**) results from two successive coordination of N_2 to the $RuH_2(PH_3)_2$ fragment (see Equation 2 in Scheme 1). The six vertices of the octahedral environment around the ruthenium atom are all occupied. Five isomers have been examined and their DFT/B3LYP optimized geometries are shown in Fig. 2. We have adopted the same numbering as above. **2Ta** and **2Tb** have the phosphines in *trans* position whereas they are in *cis* position in **2Ca**, **2Cb** and **2Cc**. In the 'a' series, (**2Ta** and **2Ca**), the two dinitrogen ligands as well as the two hydrides are in *cis* position. In the 'b' series (**2Tb** and **2Cb**), the two N_2 ligands are in *trans* position while the two hydrides are in *trans* position in **2Tb** and *cis* in **2Cb**. In **2Cc,** the two dinitrogen ligands are in *cis* position and the two hydrides are in *trans* position.

As already mentioned, it is well known that the *trans* position of two hydrides is unfavourable. We have

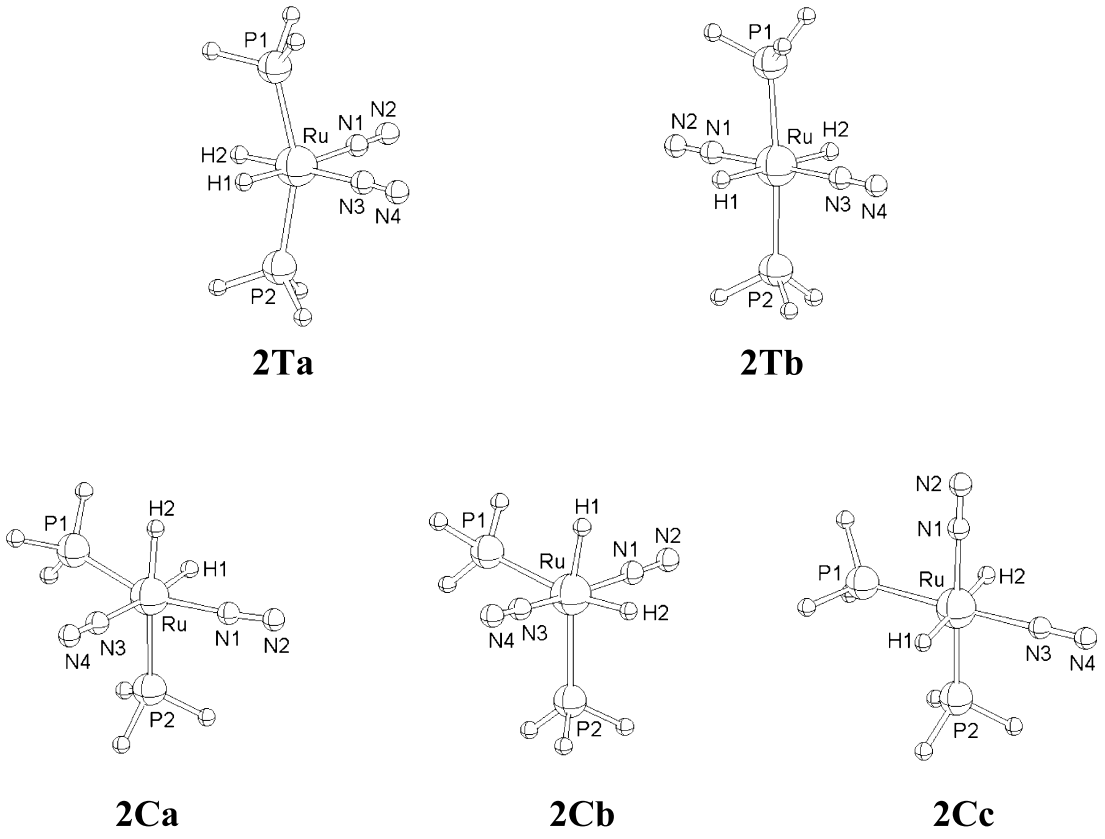

Fig. 2. DFT/B3LYP-optimized geometries of $RuH_2(N_2)_2(PH_3)_2$ isomers (**2**).

however included **2Tb** and **2Cc** in our calculations in order to verify that this statement remains true in the case of bis(dinitrogen) complex.

Optimized values of selected geometrical parameters for the five isomers are reported in Table 3. Isomers **2Ta** and **2Cb** have C_{2v} symmetry whereas isomers **2Tb** and **2Ca** have no symmetry. The relative energies as well as corrections of ZPE and thermal enthalpy are given in Table 4. Even after corrections, we can note that the three isomers **2Ta**, **2Ca** and **2Cb** are close in energy, but not strictly degenerated. **2Ta** appears to be the most stable of the series. As for the mono(dinitrogen) complexes, the *trans* position of the two phosphines is preferred. Isomer **2Ta** is calculated to be lower than **2Ca** by 3.3 kcal mol^{-1}. Isomer **2Cb** containing two dinitrogen *trans* to each other is 6.4 kcal mol^{-1} above **2Ta**. As expected, isomer **2Tb** and **2Cc** are less stable than their homologues **2Ta** and **2Ca** by about 15 and 13 kcal mol^{-1}, respectively. This confirms that a *trans* position of the two hydrides is not favourable.

The Ru–N1–N2 and Ru–N3–N4 angles are very flat. All the isomers can be described as dihydride complexes with two end-on dinitrogen ligands. On the other hand, the N–N distance has nearly the same value of 1.12 Å for all isomers. This distance can be compared with that calculated in the mono(dinitrogen) complex $RuH_2(N_2)(PH_3)_2$. It is roughly equal to the value in the **1C** series but slightly shorter than in the trans isomer **1Ta**, indicating a weak activation of the dinitrogen ligands.

Since isomers **2Ta** and **2Ca** are very close in energy, we have calculated the energy of the isomerization barrier. We have optimized the geometry of the transition structure denoted $\mathbf{TS_{TC}}$ connecting these two isomers. Only one imaginary frequency has been found (213i cm^{-1}). Compared to **2Ta** and **2Ca**, the geometry of $\mathbf{TS_{TC}}$ is characterized by a strong shortening of the H1–H2 distance from about 2.15 to 0.92 Å whereas the H1–Ru–H2 angle decreases from 82.8° to 31.2°. This geometry is compatible with the formation of a dihydrogen complex [6–10]. Note that as expected, the P1–Ru–P2 angle in $\mathbf{TS_{TC}}$ is 126.7° which is an intermediate value between those in **2Ta** and **2Ca**. The value of the isomerization barrier is 31.1 kcal mol^{-1} (Fig. 3), thus sufficiently high to render difficult the isomerization process. We have verified that $\mathbf{TS_{TC}}$ is the true transition state by calculating the variation of the electronic energy versus the IRC over the isomerization path. The potential energy profile along the mass-weighted steepest-descent isomerization path is shown in Fig. 4. The transition state is characterized by the existence of a flat domain instead of a pick as it is usually observed. This

Table 3
Selected optimized geometrical parameters [a] for $RuH_2(N_2)_2(PH_3)_2$ isomers and for $\mathbf{TS_{TC}}$ calculated at the DFT/B3LYP level of theory

	2Ta (C_{2v})	$\mathbf{TS_{TC}}$ (C_1)	**2Ca** (C_1)	**2Cb** (C_{2v})	**2Cc** (C_s)	**2Tb** (C_1)
Ru–H1	1.634	1.695	1.634	1.620	1.700	1.687
Ru–H2	1.634	1.715	1.622	1.620	1.687	1.702
Ru–N1	2.019	1.996	1.963	1.971	2.013	1.969
Ru–N3	2.019	2.097	2.018	1.971	2.013	1.969
H1–H2	2.165	0.915	2.149	2.131	3.386	3.389
N1–N2	1.124	1.121	1.123	1.119	1.118	1.120
N3–N4	1.124	1.122	1.124	1.119	1.118	1.120
Ru–P1	2.322	2.330	2.329	2.415	2.300	2.337
Ru–P2	2.322	2.335	2.406	2.415	2.300	2.337
P1–Ru–P2	157.4	126.7	96.8	103.8	91.0	175.1
H1–Ru–H2	82.8	31.2	82.9	82.3	176.0	179.9
H1–Ru–P1	82.2	84.7	82.0	87.0	86.9	92.5
H2–Ru–P1	82.2	86.5	80.2	169.2	90.5	87.6
H1–Ru–P2	82.2	78.1	86.6	87.0	86.9	92.4
H2–Ru–P2	82.2	101.7	169.7	169.2	90.5	87.6
H1–Ru–N1	174.0	158.6	86.6	86.0	91.7	89.9
H1–Ru–N3	90.0	108.9	174.2	86.0	91.7	90.2
H2–Ru–N1	174.0	168.1	86.3	86.0	90.9	90.2
H2–Ru–N3	90.0	81.9	91.0	86.0	90.9	90.2
N1–Ru–P1	97.0	88.8	163.2	93.3	89.9	90.0
N3–Ru–P1	97.0	89.8	94.3	93.3	178.3	90.1
N1–Ru–P2	97.0	123.3	96.4	93.3	178.3	90.0
N3–Ru–P2	97.0	109.8	99.2	93.3	89.9	90.0
N1–Ru–N3	98.0	91.4	96.6	169.3	89.1	179.6
Ru–N1–N2	179.4	176.9	175.4	178.0	179.9	179.6
Ru–N3–N4	179.4	179.2	177.6	178.0	179.9	179.5

[a] Distances are in angstrom (Å) and angles in degrees (°).

Table 4
DFT/B3LYP relative energies (kcal mol^{-1}) of $RuH_2(N_2)_2(PH_3)_2$ isomers

Isomer	ΔE	ΔE+ZPE	ΔH°	ΔG°
2Ta	0.0	0.0	0.0	0.0
2Tb	16.1	15.3	15.2	14.8
2Ca	3.6	3.3	3.3	3.0
2Cb	6.8	6.4	6.4	6.5
2Cc	16.8	16.1	15.9	15.8
$\mathbf{TS_{TC}}$	32.2	30.9	31.1	29.9

domain is relative to the formation of a dihydrogen molecule in the Ru-complex as a result of a geometrical rearrangement of the two hydrides.

3.3. The mixed (dihydrogen)(dinitrogen) complex $RuH_2(H_2)(N_2)(PH_3)_2$

Five isomers of $RuH_2(H_2)(N_2)(PH_3)_2$ (**3**) (see Equation 3 in Scheme 1) have been optimized at the DFT/B3LYP level. They are shown in Fig. 5. The main geometrical parameters as well as the relative energies, standard enthalpies and free energies are gathered in Tables 5 and 6, respectively. Isomers of **T** type with the phosphines in *trans* position are of C_s symmetry whereas isomers of **C** type with the phosphines in *cis* position have no symmetry. The only difference between the two isomers **3Ta** and **3Tb** is the position of the H_2 ligand with respect to the symmetry plane. In the former, H_2 is located in the symmetry plane whereas in the latter H_2 is perpendicular to this plane. Isomers of **C** type differ by the position of the H_2 ligand which can be located *trans* to one phosphine (**3Ca**), *trans* to one hydride (**3Cb**) or *trans* to the dinitrogen ligand (**3Cc**).

All the isomers are very close in energy within a range of 6 kcal mol^{-1}. As in the case of $RuH_2(N_2)(PH_3)_2$ and $RuH_2(N_2)_2(PH_3)_2$ complexes, isomers of **T** type with *trans* phosphines are more stable than the **C** ones. Isomers **3Ta** and **3Tb** corresponding to two different positions of H_2 with respect to the symmetry plane are quasi-degenerated. For isomer **3Ta**, the two hydrides and the two ligands H_2 and N_2 are located in the symmetry plane. Dinitrogen is end-on with a lengthening of 1% compared to free N_2 while dihydrogen is η^2-coordinated with a lengthening of 11.3% compared to free H_2. This increase of the H–H bond length under complexation is quite comparable to that calculated in $RuH_2(H_2)_2(PH_3)_2$ (12.5%) [9], indicating a small influence of the substitution of one dihydrogen by a dinitrogen on the activation of the other H_2.

In the **C** type isomers, the N–N bond length remains of the same order as in **3Ta**. On the contrary, the H_2

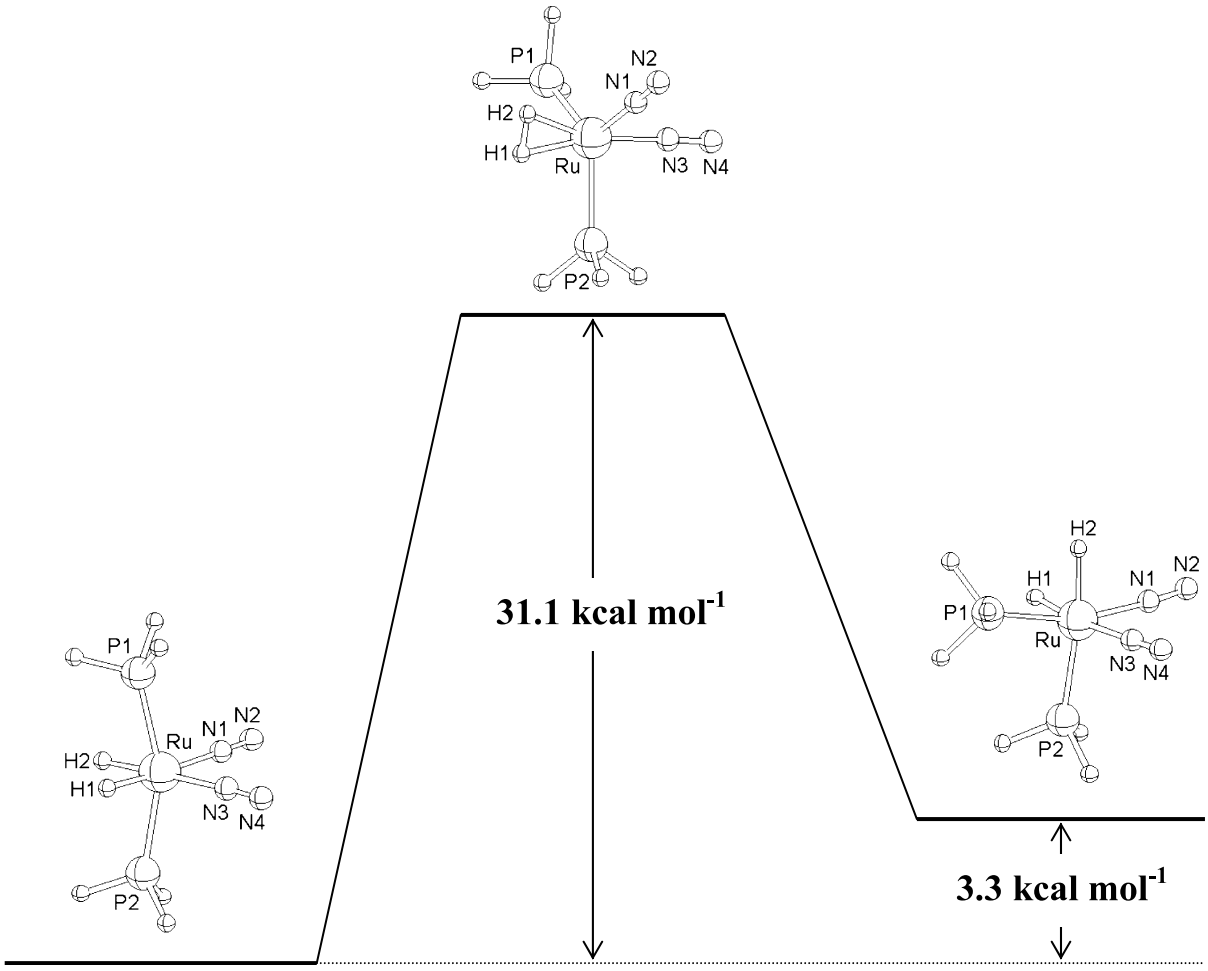

Fig. 3. Schematic energy profile for the isomerization process between the **2Ta** and **2Ca** isomers of $RuH_2(N_2)_2(PH_3)_2$.

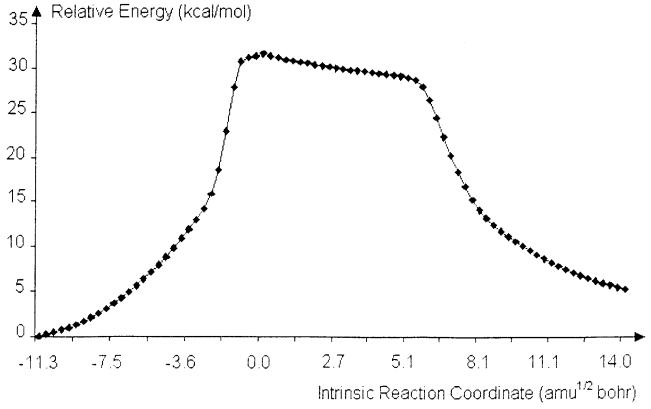

Fig. 4. DFT/B3LYP potential energy along the reaction path for the **2Ta/2Ca** isomerization process.

ligand undergoes a more important lengthening, essentially for **3Cb** (15.6%) and **3Cc** (17.9%).

3.4. Vibrational frequencies

We have mentioned in Section 1 that the complex $RuH_2(N_2)_2(PCy_3)_2$ was only characterized in solution by NMR and IR data [11]. In the absence of an X-ray determination, a comparison between IR experimental data and theoretical calculations can be performed, as the degree of activation of the N–N bond can be estimated not only by the N–N bond lengthening but also by the decrease of the ν_{NN} stretching modes. We have reported in Table 7 the frequencies of vibration for several normal modes of all the isomers.

Our B3LYP calculated value for the free N_2 stretching wave number is only 5.5% different from the experimental one. Comparatively to N_2 calculated value (2459 cm^{-1}), the value decreases more in the mono(dinitrogen) molecule (2284 cm^{-1} in **1Ta**) than in the bis-dinitrogen one (2303, 2324 cm^{-1} in **2Ta**). This is in perfect agreement with the longer bond in the former molecule (1.152 Å) than in the latter (1.124 Å). Concerning the bis(dinitrogen) complex, it is remarkable that little change is observed for the calculated values of the different isomers ($\approx$2300 and 2325 cm^{-1}). They can be compared to the two experimental ν_{NN} values of 2126 and 2163 cm^{-1}. Although the calculated data are systematically higher than experiment, the qualitative trends are remarkably similar. However, a comparison

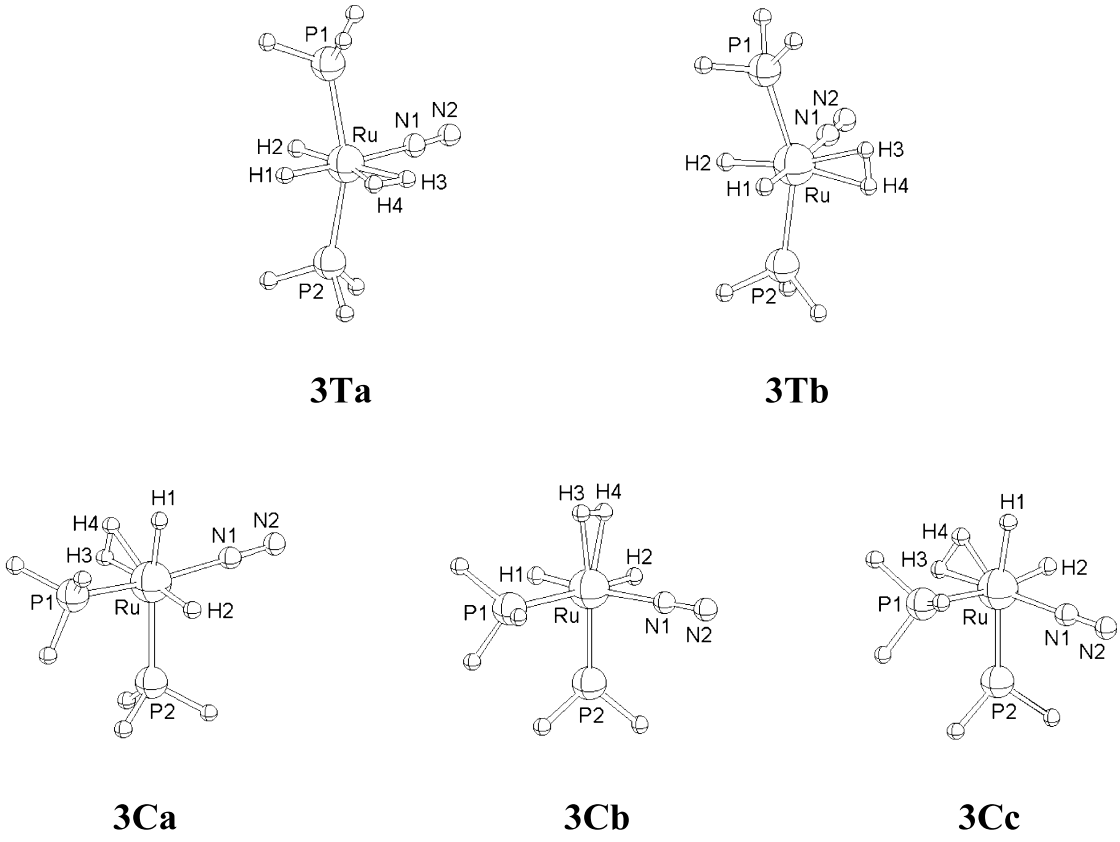

Fig. 5. DFT/B3LYP-optimized geometries of $RuH_2(H_2)(N_2)(PH_3)_2$ isomers (**3**).

of the intensities of the bands found in the experimental spectrum with the calculated values tends to favour isomer **2Ta** as the best model. It should be noted that these values might not represent pure bonding modes

Table 5
Selected optimized geometrical parameters [a] for $RuH_2(H_2)(N_2)(PH_3)_2$ isomers calculated at the DFT/B3LYP level of theory

	3Ta (C_s)	**3Tb** (C_s)	**3Ca** (C_1)	**3Cb** (C_1)	**3Cc** (C_1)
Ru–H1	1.618	1.620	1.625	1.614	1.625
Ru–H2	1.618	1.617	1.619	1.629	1.623
Ru–H3	1.835	1.823	1.819	1.763	1.725
Ru–H4	1.794	1.823	1.789	1.721	1.687
H3–H4	0.845	0.839	0.856	0.877	0.895
Ru–N1	2.070	2.063	2.008	2.074	1.987
N1–N2	1.119	1.120	1.118	1.119	1.119
Ru–P1	2.313	2.310	2.286	2.379	2.397
Ru–P2	2.313	2.310	2.390	2.292	2.390
P1–Ru–P2	161.6	155.6	96.5	96.5	104.5
H1–Ru–H2	82.3	86.3	86.6	83.6	83.5
H3–Ru–H4	26.9	26.6	27.4	29.1	30.4
H1–Ru–P1	82.8	81.8	80.7	86.3	86.6
H1–Ru–P2	82.8	81.8	166.5	83.3	168.9
H2–Ru–P1	83.4	80.5	83.3	174.4	169.9
H2–Ru–P2	83.4	80.5	85.1	79.6	85.4
H3–Ru–P1	97.2	85.7	97.2	83.8	87.5
H3–Ru–P2	97.2	112.0	88.7	170.6	83.9
H4–Ru–P1	93.7	112.0	93.8	112.5	98.9
H4–Ru–P2	93.7	85.7	116.0	147.1	108.0
N1–Ru–P1	96.2	90.7	165.1	99.1	94.2
Ru–N1–N2	176.7	178.3	177.0	178.4	178.5

[a] Distances are in angstrom (Å) and angles in degrees (°).

Table 6
DFT/B3LYP relative energies (kcal mol^{-1}) of $RuH_2(N_2)(H_2)(PH_3)_2$ isomers

Isomer	ΔE	ΔE+ZPE	ΔH°	ΔG°
3Ta	0.0	0.0	0.0	0.0
3Tb	0.6	0.5	0.6	0.2
3Ca	2.1	2.3	2.1	2.4
3Cb	2.3	2.3	2.2	2.3
3Cc	6.2	5.7	5.9	5.3

Table 7
DFT/B3LYP calculated ν_{NN} wavenumbers (cm^{-1}) and infrared intensities (km mol^{-1}) for the N–N stretching modes in $RuH_2(N_2)(PH_3)_2$, $RuH_2(N_2)_2(PH_3)_2$ and $RuH_2(H_2)(N_2)(PH_3)_2$

Compound	Isomer	Symmetry	ν_{NN}	Intensity
$RuH_2(N_2)(PH_3)_2$	**1Ta**	a	2284	433
	1Ca	a	2297	502
	1Cb	a	2296	437
	1Cc	a	2264	429
$RuH_2(N_2)_2(PH_3)_2$	**2Ta**	b_2	2303	450
		a_1	2324	275
	2Tb	a	2289	780
		a	2317	0
	2Ca	a	2311	373
		a	2331	378
	2Cb	b_1	2299	775
		a_1	2326	59
	2Cc	a″	2307	305
		a′	2330	384
	Exp. [a]		2126	s
			2163	m
$RuH_2(H_2)(N_2)(PH_3)_2$	**3Ta**	a′	2318	327
	3Tb	a′	2308	373
	3Ca	a	2322	417
	3Cb	a	2314	374
	3Cc	a	2319	316
N_2	Calc.	σ_g	2459	49
	Exp.		2331	

[a] For $RuH_2(N_2)_2(PCy_3)_2$ see Ref. [11].

and in addition, that PH_3 has been used as a model of PCy_3.

3.5. Thermodynamic analysis

3.5.1. Binding energies

We have calculated successive bonding energies of N_2 on the $RuH_2(PH_3)_2$ fragment. We will call $\Delta_r E$ the energy difference associated with the equations 1 and 2 shown in Scheme 1. ZPE, thermal enthalpies ($\Delta_r H^\circ$) and Gibbs free energies ($\Delta_r G^\circ$) corresponding to equations (1) and (2) at the standard conditions (298.15 K and 1 atm) were obtained from the vibrational frequency calculations for **1Ta** and **2Ta**. Results are summarized in Table 8.

Table 8
Predicted binding energies (kcal mol^{-1}) of N_2 calculated with different methods at the DFT/B3LYP optimized geometries

		Eq. 1	Eq. 2
$\Delta_r E$	HF	−2.6	−4.5
	MP2	−25.6	−24.7
	MP3	−11.1	−11.8
	MP4SDQ	−23.4	−23.4
	CCSD	−16.2	−16.6
	CCSD(T)	−19.5	−19.2
	DFT/B3LYP	−19.8	−16.8
$\Delta_r E$+ZPE	DFT/B3LYP	−17.3	−14.4
$\Delta_r H^\circ$	DFT/B3LYP	−18.0	−14.9

The DFT/B3LYP $\Delta_r E$ energy for the coordination of one dinitrogen molecule on the $RuH_2(PH_3)_2$ fragment is 19.8 kcal mol^{-1}. For the second N_2 coordination, the $\Delta_r E$ value is slightly lower by 3 kcal mol^{-1}. The $\Delta_r H^\circ$ values present the same tendency. It should be noted that these values should be corrected from the effect of basis set superposition errors. We have previously observed a small reduction of binding energy values using such corrections in the case of bis(silane) complexes [19,20]. These binding energies of N_2 can be compared with those calculated for H_2 coordinated to the same metallic fragment using the same theoretical procedure ($\Delta_r E$ values of 17.6 kcal mol^{-1} for the complexation of the first H_2 and 18.1 kcal mol^{-1} for the second) [19]. We can conclude that the dinitrogen ligand in the most stable isomers is not more strongly bound than dihydrogen. This is consistent with the fact that the preparation of $RuH_2(N_2)_2(PR_3)_2$ by displacement of molecular H_2 from $RuH_2(H_2)_2(PR_3)_2$ is easily reversible.

In order to testify the quality of our calculation method (DFT/B3LYP), we have also calculated the $\Delta_r E$ binding energies using different methods at the B3LYP-optimized geometry (see Table 8). We intend to compare our results assuming that the values calculated with the sophisticated CCSD(T) method can be considered as the most accurate. Compared to CCSD(T), the Hartree-Fock method which does not take into account the electronic correlation energy, leads to greatly underestimated values. On the contrary, methods which include a perturbative treatment of the electronic correlation such as MP2 or MP4SDQ can lead to overestimated values. This emphasises the necessity of a more accurate treatment of the electronic correlation in order to get some reasonable values. We can see that, in the case of the complexation of the first N_2 ligand, the use of the B3LYP density functional gives values comparable to those obtained by the CCSD(T) method.

However, whereas the CCSD(T) method deals with a binding energy for the second ligand nearly equal to the one of the first ligand, the DFT/B3LYP value for the second ligand is slightly weaker. Nevertheless, the DFT/B3LYP method appears to be the best one for estimating the binding energies.

3.5.2. Substitution reactions on $RuH_2(H_2)_2(PH_3)_2$

Experimental studies have shown that dihydrogen substitution by dinitrogen is achieved by bubbling dinitrogen to a pentane suspension of $RuH_2(H_2)_2(PCy_3)_2$. The bis(dinitrogen) complex $RuH_2(N_2)_2(PCy_3)_2$ was characterized by NMR and IR data [11]. The reaction is reversible since it is possible to regenerate the initial complex under a dihydrogen atmosphere. Intuitively, we cannot eliminate the possibility to have a complex that contains both H_2 and N_2 ligands. We have thus calculated the energy differences corresponding to the substitution of one and two dihydrogen ligands by one and two dinitrogen within the model complex $RuH_2(H_2)_2(PH_3)_2$. The reactions are described in Scheme 2 and the thermodynamic quantities are gathered in Table 9. As shown by the Δ_rG° values, all close to zero, the three reactions are reversible. This is in complete agreement with the experimental observations.

3.6. NBO analysis

The NBO analysis allows the evaluation of the various electron transfers occurring between the metal and the dinitrogen ligand in the complexes. We have reported in Table 10 the natural charges q, the Wiberg bond indices W and the natural orbital occupancies for the most stable isomers of $RuH_2(N_2)(PH_3)_2$ (**1Ta**), $RuH_2(N_2)_2(PH_3)_2$ (**2Ta**) and $RuH_2(H_2)(N_2)(PH_3)_2$ (**3Ta**) as well as for free N_2.

An evaluation of the charge of the N_2 ligand can be easily obtained by summing the two individual charges on both nitrogen atoms. It occurs that the values are all close to zero (-0.08 for **1Ta**, -0.14 for **2Ta** and -0.03 for **3Ta**), showing that no noticeable global charge transfer between N_2 and the ruthenium fragment occurs under complexation.

Analyzing the Ru–H Wiberg bond indices for the three complexes, we note that the same value (~ 0.65) has been obtained except for the Ru–H2 bond of the mono(dinitrogen) complex (**1Ta**) in which this hydride is *trans* to the vacant site. In that case, the bond index is higher for Ru–H2 than for Ru–H1 (0.86 versus 0.65). This observation is confirmed by the shortness of the Ru–H2 bond (1.651Å) compared to the Ru–H1 bond (1.666Å) (see Table 1). The Wiberg index of the N_2 bond is reduced in the three complexes, with a decrease of approximately 0.20 compared to free N_2 (bond index of 3 corresponding to a triple bond). This is in agreement with the very short elongation of the N–N bond observed in the complexes relatively to free N_2.

We have represented in Fig. 6 the orbital diagram showing the interactions between the metallic fragment $RuH_2(PH_3)_2$ and dinitrogen. End-on bonding can be commonly described as the result of two electron transfers. First this binding mode involves a σ-donation from the N_2 $2\sigma_g$ orbital to the LUMO orbital 8a′* of $RuH_2(PH_3)_2$. On the other hand, the three highest occupied orbitals of the metallic fragment (5a″, 6a″

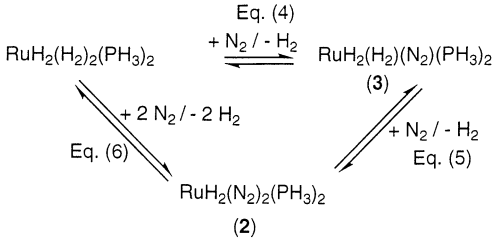

Scheme 2.

Table 9
Thermodynamic data (kcal mol^{-1}) for the substitution of dihydrogen by dinitrogen in $RuH_2(H_2)_2(PH_3)_2$ calculated at the DFT/B3LYP level of theory

	Δ_rE	Δ_rE+ZPE	Δ_rH°	Δ_rG°
Eq. (4) [a]	0.3	−0.1	−0.6	0.6
Eq. (5) [a]	−0.8	−1.3	−1.8	0.1
Eq. (6) [a]	−0.6	−1.4	−2.4	0.7

[a] See Scheme 2.

Table 10
Selected natural charges q, Wiberg bond indices W, and natural orbital occupancies of N_2, $RuH_2(N_2)(PH_3)_2$ (**1Ta**), $RuH_2(N_2)_2(PH_3)_2$ (**2Ta**) and $RuH_2(H_2)(N_2)(PH_3)_2$ (**3Ta**) calculated at the DFT/B3LYP level of theory

	N_2	**1Ta**	**2Ta**	**3Ta**
q(Ru)		−0.44	−0.44	−0.63
q(H1)		0.07	−0.07	−0.07
q(H2)		−0.14	−0.07	−0.04
q(H3)				0.07
q(H4)				0.04
q(N1)	0.0	−0.09	−0.07	−0.06
q(N2)	0.0	0.01	−0.07	0.03
q(P)		0.34	0.37	0.37
W(Ru–H1)		0.65	0.65	0.63
W(Ru–H2)		0.86	0.65	0.63
W(Ru–N1)		0.45	0.39	0.39
W(H3–H4)				0.71
W(N1–N2)	3.02	2.76	2.80	2.80
σ(H3–H4)				1.78
Lp(N1) [a]	1.99	1.79	1.80	1.79
Lp(N2) [a]	1.99	1.98	1.98	1.98
σ*(H3–H4)				0.09
π_g^*(N1–N2)	0.00	0.13	0.11	0.11

[a] Lp, lone pair. See Figs. 1, 2 and 5 for labeling of the atoms.

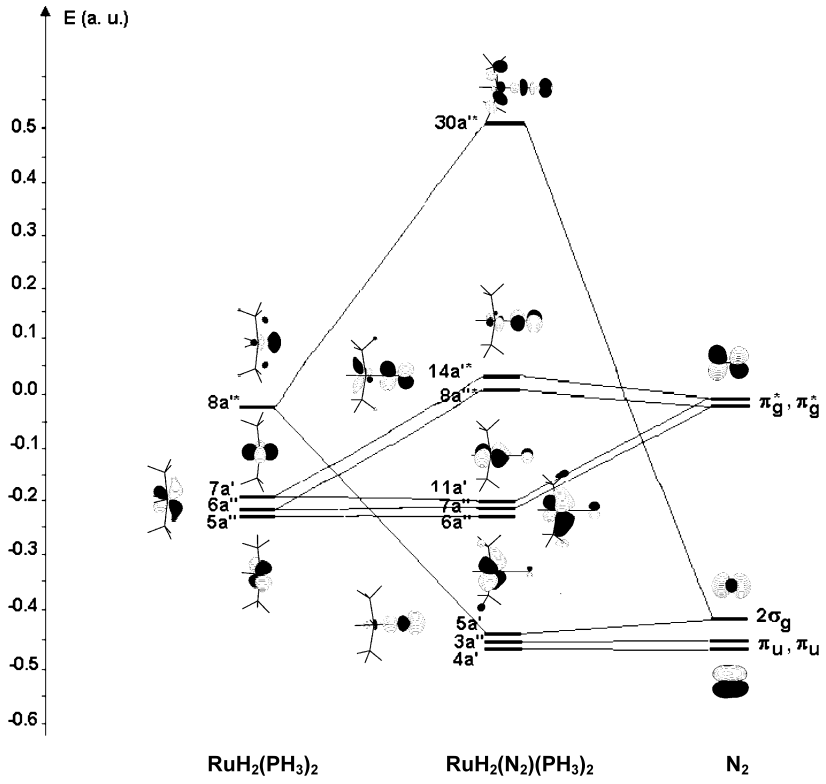

Fig. 6. Orbital interaction diagram for the formation of $RuH_2(N_2)(PH_3)_2$ (**1Ta**).

and 7a′) are mainly 4d ruthenium orbitals. Two of them are involved in a π back-bonding from the metal to the N_2 π_g^* orbitals. The relative values of these two transfers can be deduced from the orbital occupancies in the NBO description. In the three complexes **1Ta**, **2Ta** and **3Ta**, the N1 lone pair lost 0.20 electron with respect to free dinitrogen, meanwhile the N2 lone pair remained unchanged. The N_2 π_g^* orbitals present a total occupancy of 0.26 electron for **1Ta** and 0.22 electron for **2Ta** and **3Ta**. This result which is coherent with a very small global charge transfer indicates that back-bonding is of the same order as σ-donation. Similar analysis have been reported on a series of iron [21] and tungsten [22] carbonyl complexes.

The case of the mixed complex **3Ta** allows comparing the bonding nature of one dihydrogen and one dinitrogen coordinated to the same ruthenium atom. For the η^2-H_2 bond, while the σ-donation from the dihydrogen σ bond orbital to the $RuH_2(PH_3)_2$ orbital involves also 0.22 electron, the back-bonding from the occupied 4d orbital of Ru to the σ* orbital of H_2 concerns only 0.09 electron. In that case, σ-donation is more important with back-bonding occurring to a lesser degree. We have shown that in **3Ta**, the lengthening of H_2 under complexation is 11.3% greater than in free H_2 whereas only 1% lengthening of N_2 versus free N_2 is calculated. This can be easily explained by the different nature of the orbitals involved in the σ-donation. In the case of H_2, a σ-bonding orbital is involved, as opposed to a mainly nonbonding orbital i.e., the $2\sigma_g$ orbital shown in Fig. 6, for N_2.

4. Conclusion

In this work, we have investigated the complexation of dinitrogen on ruthenium atom. In all the isomers, the dinitrogen is coordinated to the metal in an end-on bonding mode. In the most stable isomers, the phosphines are in *trans* position while the dinitrogen molecule is *trans* to one hydride. The dinitrogen bond length elongation was found very short approximately 1%, for most of the calculated isomers (except for **1Ta** ~4%). It is noteworthy that for the bis(dinitrogen) complex $RuH_2(N_2)_2(PH_3)_2$, the most stable isomer **2Ta** has the same geometry as the one found for the corresponding bis(dihydrogen) complex, both theoretically for $RuH_2(H_2)_2(PH_3)_2$ [9] and experimentally for $RuH_2(H_2)_2(PCy_3)_2$ [10]. Moreover, the binding energies of N_2 are of the same order as the ones found for H_2 coordination to the same metal fragment. The free energy values corresponding to the substitution of H_2 by N_2 are close to zero. This is in agreement with the reversible substitution of H_2 by N_2 in $RuH_2(H_2)_2(PCy_3)_2$ as observed experimentally [11]. It is rather remarkable that in these dinitrogen isomers, NBO analysis indicates that back-donation plays about the same role as σ-donation, both effects being relatively weak. Data

obtained on **3Ta** allow a direct comparison between dinitrogen and dihydrogen coordination. Coordination of H_2 with a η^2-mode results in a noticeable elongation of the H–H bond, whereas a very small elongation is associated to the end-on coordination mode of N_2. In the case of dinitrogen complexes, IR values better reflect the electronic variation within the coordinated N_2 ligand. It is noteworthy that in our ruthenium system, the dinitrogen and dihydrogen species display similar properties as also illustrated experimentally.

Acknowledgements

This work is supported by the CNRS. We thank the CINES (Montpellier, France) for a generous allocation of computer time.

References

[1] G.J. Leigh, N. Winterton, Modern Coordination Chemistry, the Legacy of Joseph Chatt (sections E and F), RSC, UK, 2002.
[2] A.D. Allen, C.V. Senoff, Chem. Comm. (1965) 621.
[3] M.D. Fryzuk, S.A. Johnson, Coord. Chem. Rev. 200–202 (2000) 379.
[4] M. Hidai, Y. Mizobe, Chem. Rev. 95 (1995) 1115.
[5] S. Gambarotta, J. Organomet. Chem. 500 (1995) 117.
[6] P.G. Jessop, R.H. Morris, Coord. Chem. Rev. 121 (1992) 155.
[7] G.J. Kubas, Metal Dihydrogen and σ-Bond Complexes, Kluwer Academic/Plenum Publishers, New York, 2001.
[8] (a) S. Sabo-Etienne, B. Chaudret, Coord. Chem. Rev. 178–180 (1998) 381;
(b) V. Montiel-Palma, M. Lumbierres, B. Donnadieu, S. Sabo-Etienne, B. Chaudret, J. Am. Chem. Soc. 124 (2002) 5624 (references therein);
(c) I. Atheaux, F. Delpech, B. Donnadieu, S. Sabo-Etienne, B. Chaudret, K. Hussein, J.-C. Barthelat, T. Braun, S.B. Duckett, R.N. Perutz, Organometallics 21 (2002) 5347.
[9] V. Rodriguez, S. Sabo-Etienne, B. Chaudret, J. Thoburn, S. Ulrich, H.-H. Limbach, J. Eckert, J.-C. Barthelat, K. Hussein, C.J. Marsden, Inorg. Chem. 37 (1998) 3475.
[10] (a) A.F. Borowski, B. Donnadieu, J.-C. Daran, S. Sabo-Etienne, B. Chaudret, Chem. Commun. (2000) 543.;
(b) A.F. Borowski, B. Donnadieu, J.-C. Daran, S. Sabo-Etienne, B. Chaudret, Chem. Commun. (2000) 1697.
[11] (a) S. Sabo-Etienne, M. Hernandez, G. Chung, B. Chaudret, New J. Chem. 18 (1994) 175;
(b) M.L. Christ, S. Sabo-Etienne, G. Chung, B. Chaudret, Inorg. Chem. 33 (1994) 5136.
[12] K. Abdur-Rashid, D.G. Gusev, A.J. Lough, R.H. Morris, Organometallics 19 (2000) 1652.
[13] M.J. Frisch, G.W. Trucks, H.B. Schlegel, G.E. Scuseria, M.A. Robb, J.R. Cheeseman, V.G. Zakrzewski, J.A. Montgomery, Jr., R.E. Stratmann, J.C. Burant, S. Dapprich, J.M. Millam, A.D. Daniels, K.N. Kudin, M.C. Strain, O. Farkas, J. Tomasi, V. Barone, M. Cossi, R. Cammi, B. Mennucci, C. Pomelli, C. Adamo, S. Clifford, J. Ochterski, G.A. Petersson, P.Y. Ayala, Q. Cui, K. Morokuma, P. Salvador, J.J. Dannenberg, D.K. Malick, A.D. Rabuck, K. Raghavachari, J.B. Foresman, J. Cioslowski, J.V. Ortiz, A.G. Baboul, B.B. Stefanov, G. Liu, A. Liashenko, P. Piskorz, I. Komaromi, R. Gomperts, R.L. Martin, D.J. Fox, T. Keith, M.A. Al-Laham, C.Y. Peng, A. Nanayakkara, M. Challacombe, P.M.W. Gill, B. Johnson, W. Chen, M.W. Wong, J.L. Andres, C. Gonzalez, M. Head-Gordon, E.S. Replogle, J.A. Pople, GAUSSIAN 98, Revision A.11, Gaussian, Inc., Pittsburgh PA, 2001.
[14] (a) A.D. Becke, J. Chem. Phys. 98 (1993) 5648;
(b) C. Lee, W. Yang, R.G. Parr, Phys. Rev. B 37 (1988) 785.
[15] (a) K. Hussein, C.J. Marsden, J.-C. Barthelat, V. Rodriguez, S. Conejero, S. Sabo-Etienne, B. Donnadieu, B. Chaudret, Chem. Commun. (1999) 1315;
(b) F. Delpech, S. Sabo-Etienne, J.C. Daran, B. Chaudret, K. Hussein, C.J. Marsden, J.-C. Barthelat, J. Am. Chem. Soc. 121 (1999) 6668;
(c) I. Atheaux, B. Donnadieu, V. Rodriguez, S. Sabo-Etienne, B. Chaudret, K. Hussein, J.-C. Barthelat, J. Am. Chem. Soc. 122 (2000) 5664.
[16] P. Durand, J.-C. Barthelat, Theor. Chim. Acta 38 (1975) 283.
[17] Y. Bouteiller, C. Mijoule, M. Nizam, J.-C. Barthelat, J.-P. Daudey, M. Pélissier, B. Silvi, Mol. Phys. 65 (1988) 2664.
[18] A.E. Reed, L.A. Curtiss, F. Weinhold, Chem. Rev. 88 (1988) 899.
[19] K. Hussein, Ph.D. Thesis, Université Paul Sabatier, Toulouse, France, 2000.
[20] S.S. Xantheas, J. Chem. Phys. 104 (1996) 8821.
[21] U. Radius, F.M. Bickelhaupt, A.W. Ehlers, N. Goldberg, R. Hoffmann, Inorg. Chem. 37 (1998) 1080.
[22] A. Kovacs, G. Frenking, Organometallics 20 (2001) 2510.